nature materials

LETTERS

PUBLISHED ONLINE: 9 MARCH 2014 | DOI: 10.1038/NMAT3901

Three-dimensional broadband omnidirectional acoustic ground cloak

Lucian Zigoneanu, Bogdan-Ioan Popa and Steven A. Cummer*

The control of sound propagation and reflection has always been the goal of engineers involved in the design of acoustic systems. A recent design approach based on coordinate transformations, which is applicable to many physical systems[1–14], together with the development of a new class of engineered materials called metamaterials, has opened the road to the unconstrained control of sound. However, the ideal material parameters prescribed by this methodology are complex and challenging to obtain experimentally, even using metamaterial design approaches. Not surprisingly, experimental demonstration of devices obtained using transformation acoustics is difficult, and has been implemented only in two-dimensional configurations[10,15]. Here, we demonstrate the design and experimental characterization of an almost perfect three-dimensional, broadband, and, most importantly, omnidirectional acoustic device that renders a region of space three wavelengths in diameter invisible to sound.

It is well understood that, given an arbitrary geometric transformation of a sound field, the effective mass density and the bulk modulus required to implement that transformation is determined as[5,16]: $\overline{\overline{\rho}}^{\,r} = \det(A)(A^{-1})^T \overline{\overline{\rho}}^{\,v} A^{-1}$ and $B^r = \det(A)B^v$, where $\overline{\overline{\rho}}$ is the mass density tensor, B is the bulk modulus, A is the Jacobian matrix of the transformation and r and v denote the real and virtual space, respectively. One application of the coordinate transformation method that received significant attention, and that we focus on here, is the so-called ground cloak. The ground cloak is a material shell that when placed over arbitrary objects sitting on reflecting surfaces, that is ground, makes the object undetectable using sound radiation. The concept has been introduced in the context of electromagnetics[17–19], but has rapidly been extended to other physical systems, including acoustics[10].

The coordinate transformation technique enabling these cloaking devices is especially suitable for acoustics. Developed in its full three-dimensional (3D) form by demonstrating the isomorphism of the acoustic wave equation and the conductivity equation[5], the method requires a wide range of anisotropic and inhomogeneous material parameters. Unlike electromagnetics, however, these properties are easier to realize in acoustics in a broadband manner using metamaterial methods because conventional materials have a broad range of acoustic material parameters spanning multiple orders of magnitude.

There have been attempts to avoid the difficulties associated with the coordinate transformation approach by using different scatter reduction techniques[20,21]. However, these other approaches have their own challenges, which have led to reduced functionality (for example, unidirectional as opposed to omnidirectional) experimental implementations. Here we show that omnidirectional 3D ground cloaks obtained using coordinate transformation methods are feasible in practice.

There are several options for geometric transformations that will map the volume occupied by the object to hide into a flat region. The so-called quasi-conformal map[8,17,19] results in isotropic material parameters but requires a cloaking shell many times larger than the object to be hidden. A simple unidirectional transformation[22–25] results in a much more compact cloaking shell but requires strongly anisotropic effective material properties. This is the design approach we take.

The geometry and transformation are depicted in Fig. 1, where the object that we want to hide is a square pyramid placed on a reflecting surface. The entire cloaked space is split into four separate quadrants. We find a proper transformation for each of them. For example, for the region characterized by $y \geqslant |x| \geqslant 0$, that is, the cut-out region shown in the top panel of Fig. 1, a suitable transformation that results in homogeneous material parameters is: $u = x, v = y$, $w = (c/(c-a))((a/b)|y| + (z-a))$, where (x, y, z) are the coordinates in the real space and (u, v, w) are the coordinates of the virtual space. The constants a, b and c are the pyramidal object dimensions given in Fig. 1, namely $a = 5.7$ cm is the object height, $c = 11.4$ cm is the cloaked region height and $b = 17.15$ cm is half the pyramid base width.

Following the transformation procedure, the material parameters required by the ideal cloak are $\rho_{11}^{pr} = 2.28$, $\rho_{22}^{pr} = 0.5$, $\rho_{33}^{pr} = 0.44$ and $B^{pr} = 0.5$, where pr denotes the principal components (eigenvalues) of the mass density tensor and bulk modulus. The orientation of the principal axes relative to the original coordinate system xyz is the same inside each quadrant, but varies from quadrant to quadrant. For example, for the same region that has the transformation specified above, the principal axis labelled 3 is parallel to the Ox axis, and the principal axis 2 is in the yOz plane and makes a 23° angle with the Oy axis. Principal axis 1 is perpendicular on the plane formed by 2 and 3. These material parameters are relative to the background material parameters, which is air in our case. A material that is less dense and more compressible than air is difficult to obtain with passive acoustic metamaterials.

However, if we begin the design procedure with a pyramidal object in a virtual space that has relative (to air) density and bulk modulus of m (called scaling factor) times higher than for air, then we find the cloaking shell parameters are $\rho_{11}^{pr,new} = m\rho_{11}^{pr}$, $\rho_{22}^{pr,new} = m\rho_{22}^{pr}$, $\rho^{pr,new}c_{33} = m\rho_{33}^{pr}$ and $B^{pr,new} = mB^{pr}$. For $m = 2.5$, all of the material parameters required by the cloaking can be realized using passive acoustic metamaterials. This change has the effect of making the cloaked object behave like a pyramid of relative density and bulk modulus of 2.5 instead of air (as depicted in Fig. 1). This is an object with the same sound velocity as air but with a modest impedance

Department of Electrical and Computer Engineering, Duke University, North Carolina 27708, USA. *e-mail: cummer@ee.duke.edu

© 2014 Macmillan Publishers Limited. All rights reserved.

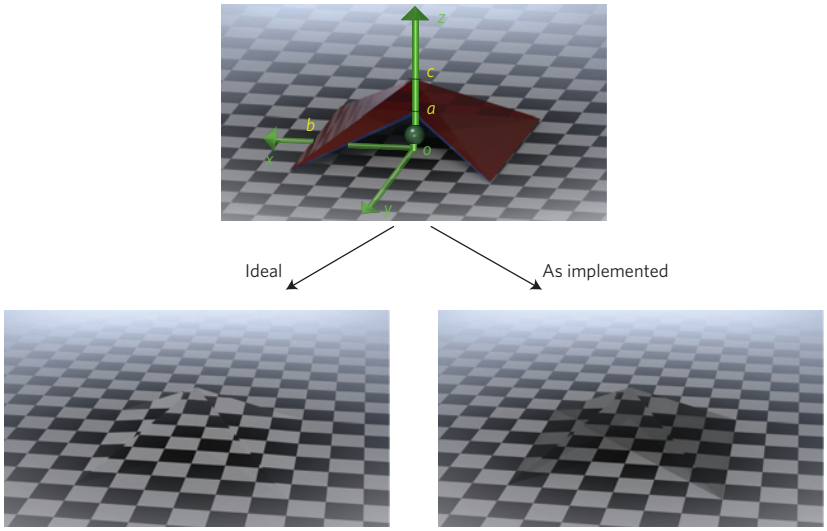

Figure 1 | Schematic representation of the pyramid-shaped acoustic ground cloak. The cloak (red region) was designed to cover, at 3 kHz, a hollow square pyramid (blue thin sheet) 34.3 cm (3λ) long and 5.7 cm tall (0.5λ), placed on the ground. λ is the wavelength in air at the design frequency. The cloak shares the same base with the object we wanted to hide and extends in the vertical direction from 5.7 cm (0.5λ) to 11.4 cm (λ). One-quarter of the cloak is removed to highlight that any object (for example, the green sphere) could be placed inside. The bottom panels qualitatively illustrate the expected performance of the ground cloak with the ideal (perfect) and fabricated (imperfect but good) material parameters.

mismatch and thus small reflection at the interface with air[10]. Numerical simulations, shown in Supplementary Methods Section II, reveal that, indeed, an object characterized by bulk modulus and mass density 2.5 times higher than those of air causes very little scattering and is hardly detectable under normal and oblique insonifications.

For this design, two principal components of the mass density tensor have close values; thus, a similar unit cell as for the 2D cloak reported in ref. 10 can be used. The unit cell is a 5 mm air-filled cube that has in the middle an acrylic perforated plate of 1.6 mm thickness and 0.85 mm hole radius. These dimensions determine the mass density components (the higher value for the wave propagating perpendicular to the plate and the lower values for the wave propagating parallel to the plate). The unit cell is about 23 times smaller than the wavelength at the design frequency, 3 kHz; therefore, the homogenization theory holds. Further investigations of this unit-cell behaviour[10] showed that the acoustic transmission losses are modest and its effective material parameters (mass density and bulk modulus) are relatively constant for frequencies up to 6 kHz. The metamaterial structure obtained by replicating these unit cells is a medium of parallel perforated plates. The metamaterial principal axis is determined for each region of the cloak using the same procedure as described in ref. 10. The principal axis direction imposed the angle of 23° made by the perforated plates with the horizontal plane. All of the perforated plates were made using a universal laser cutting machine and clear cast acrylic sheets. Other solids with the same dimensions could be used for this design, with similar results due to the high impedance contrast between them and the air background.

The resulting cloak covering the object is presented in Fig. 2. As can be seen, the object that we want to hide is hollow and consists only of one layer of plain (that is, not perforated) acrylic sheet. There is virtually no difference between a solid pyramid and a hollow pyramid. This was confirmed by other experiments (not shown here) performed in a 1D acoustic waveguide and which compared the reflection of several nearly perfect acoustic reflectors (for example, multiple layers of acrylic sheets, thin/thick aluminium plates, multiple types of wood and so on). We performed numerical simulations to confirm that the inherent fabrication errors (for example, larger/smaller holes than desired or slightly different unit-cell dimensions due to errors in positioning the perforated plates) do keep the effective material parameters close to the desired values (that is, errors smaller than 20%).

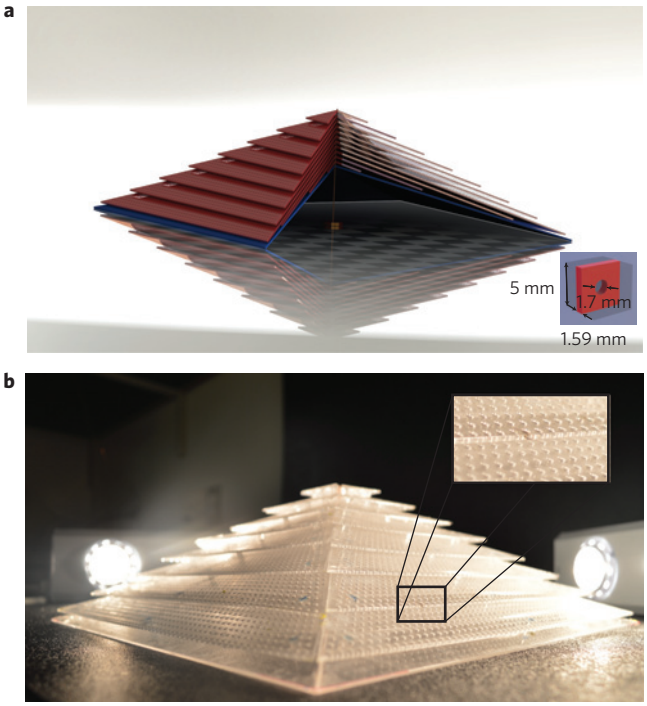

Figure 2 | Snapshots of the fabricated cloak. a, Physical structure of the designed cloak and unit-cell dimensions. One-quarter is not shown to highlight the cross-sectional view and the holding support. **b**, Photograph of the actual cloaked object, placed on the ground. Inset: details of the perforated plates. The perforations are made using a laser cutting machine and clear cast acrylic sheets.

© 2014 Macmillan Publishers Limited. All rights reserved.

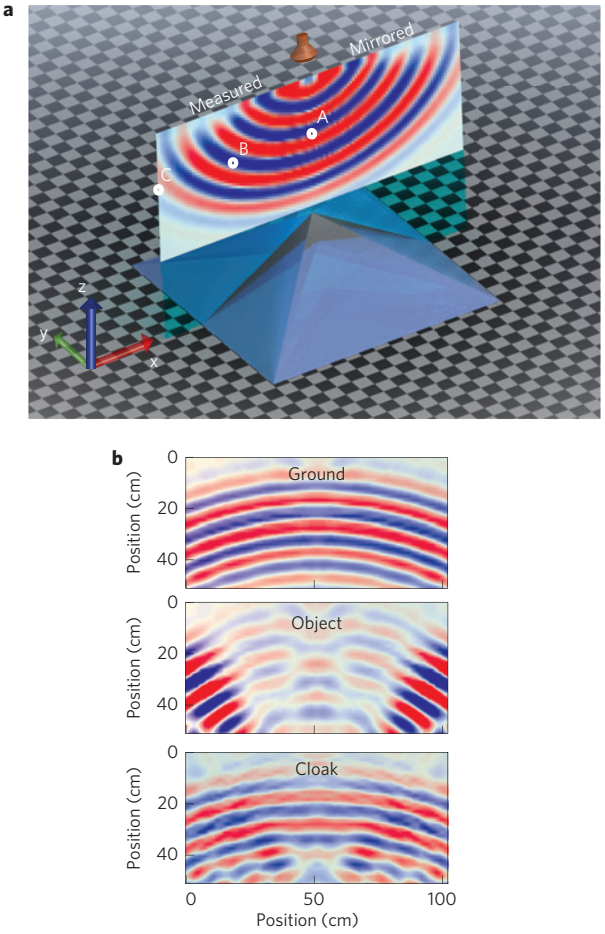

Figure 3 | Experimental set-up and qualitative results. a, Experimental set-up schematic diagram. The scanned area is 50 cm wide and 50 cm tall. This region was selected such that the cloaking effect could be clearly identified (that is, the attenuation due to free-space travel of the wave is minimal). The scanning microphone is moving on a square grid that ensures at least four measurement points per wavelength, in both directions. A, B and C are three particular measurement locations. **b**, Instantaneous scattered pressure field snapshot that highlights the object-alone acoustic signature and how the cloaked object mimics the empty ground. These plots contain the measured region and a mirrored region, to cover a larger section. A motion picture showing the incident and scattered pressure fields is presented in Supplementary Movie 1.

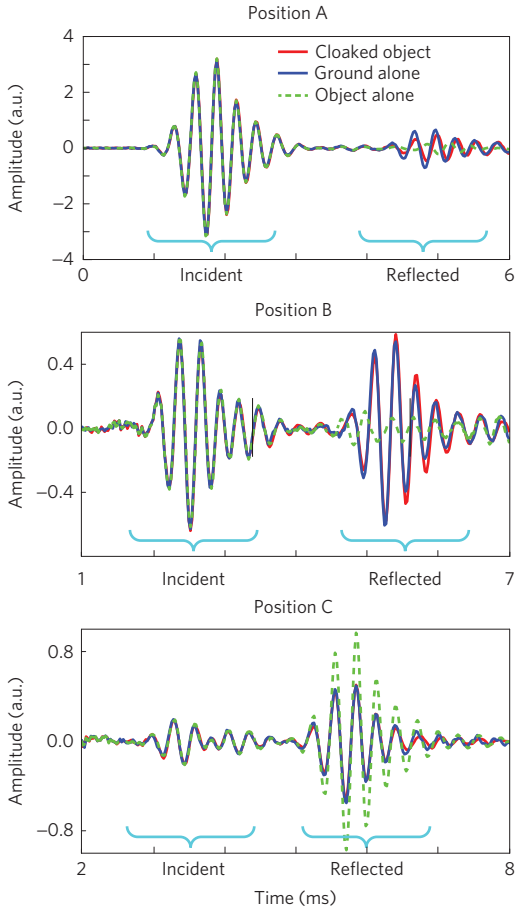

Figure 4 | Measured signals at three different locations, A, B and C. The exact location of these examples is specified in Fig. 3a. Each plot shows the incident and scattered acoustic pressure for three scenarios: empty ground, object placed on the ground and cloaked object placed on the ground.

To evaluate the performance of our device, we constructed the experimental set-up presented in Fig. 3. An almost omnidirectional sound source was set to send a short, therefore broadband, sound pulse towards the tip of the pyramidal object and perpendicularly towards the ground. This illumination was chosen to test the absolute performance of the cloak, as the incident wave hits the most uneven part of the object and cloaking device. The object and cloaking device have sharp edges in this region, and the cloaking metamaterial has discontinuities in the direction of the material principal axis; therefore, the scattering is maximized in this configuration. As we will see next, even for this unfavourable wave incidence, the cloaking shell performs almost perfectly.

Three cases were measured: with nothing on the ground (the ideal case), with only the object on the ground, and with the cloaked object on the ground, respectively. The incident sound[26] is a short Gaussian pulse of 600 μs half-amplitude duration modulated with a 3 kHz sinusoidal; that is, the pulse half-amplitude duration is slightly less than two periods. The bandwidth of this pulse, defined as the ratio between the half-amplitude band to the centre frequency of 3 kHz, is 42%. Two microphones were used to measure the acoustic wave propagation. The first one was placed in a fixed position and was used as a time reference and the other one scanned a specific region above the cloak. The planar area in which the sound is measured in this set-up is shown in Fig. 3 together with an actual measurement of the sound produced by the source. At every measurement location, several measurements are performed and averaged to increase the signal-to-noise ratio. As can be seen from the figure, the source is quasi-omnidirectional and sends waves characterized by wavevectors spanning a 28 degree sector that contains the object as seen from the source. The goal of this experimental set-up was to qualitatively and quantitatively demonstrate that the acoustic signature of the object alone is significantly minimized when it is covered with the cloak.

The instantaneous reflected pressure fields for the three cases are shown in Fig. 3. As already mentioned, the direction of the incident sound pulse was chosen so that the pulse impinges on the tip of the pyramidal object and cloaking shell, in the region with most sharp edges, where the cloaking device has discontinuities in the material principal axis. This is the situation that produces the most scattering and, therefore, the case in which the object is most visible. Figure 3b confirms this analysis. The top panel shows the expected specular reflection off the bare ground in the form of a spherical wavefront. In contrast, the object significantly disturbs this spherical field distribution. Its sharp edges generate discontinuities in the reflected wave phase profile at the horizontal positions of 25, 50 and

© 2014 Macmillan Publishers Limited. All rights reserved.

75 cm, as well as reduced backscattering towards the source and, at the same time, enhancement of the reflected field in the directions that correspond to specular reflections from the object flat faces.

Remarkably, the cloaked object reflects nearly identical to the flat reflecting plane (the bottom panel in Fig. 3b). Thus, the reflected phase front returns to the uniform spherical shape as if no object is placed in between the source and ground. The wave amplitude distribution is almost identically recovered as well, except for modest attenuation that we attribute to losses in the perforated sheets used to construct the shell. A notable aspect of this experimental result is that it agrees very well with the theoretical predictions given by the transformation acoustics theory, and, yet, it is counter-intuitive in that sharp edges and material parameter discontinuities in the metamaterial structure allow an almost perfect recovery of the ideal fields scattered by the bare ground. An animation of the instantaneous wave propagation emphasizes this result and is available in Supplementary Movie 1. To thoroughly confirm the omnidirectionality and effectiveness of the cloaking shell, several additional scanning planes and angles of incidence have been considered. All of these measurements show a substantial reduction of the scattering characteristics of the cloaked object compared with the uncloaked object. A detailed description of the measurements is included in Supplementary Methods Section III, and as Supplementary Movies 2–6.

To quantitatively show the cloak performance, we accompany the previous experimental results with a set of individual time domain measurements (Fig. 4) taken at specific points, labelled A, B and C in Fig. 3a. The time domain sound wave recorded at position A (see the top panel of Fig. 4) corresponds to the backscattering direction. The plot shows the incident short Gaussian pulse, together with the reflection from the ground reflector, bare object and cloaked object. As expected, the incident pulses are identical in all three cases. Remarkably, the phase of the wave reflected by the cloaking device is within 15° of the ideal phase, and the amplitude is 74% of the ideal amplitude, in stark contrast with the difference between the wave reflected by the object and the ideal wave form (phase difference of approximately −90°, and an amplitude ratio of 33%). Position B corresponds to the direction in which the wave reflected by the bare object is minimum, whereas position C corresponds to the direction in which the specular reflection from the object faces are maximum. In both cases, the cloaking shell almost perfectly corrects the pulse phase advance and, at the same time, brings the amplitude up or down to match it with the ideal fields.

The designed and fabricated 3D reflecting plane cloak performs well and demonstrates that the design methodology used is a robust one. These experimental results provide a clear path for realizing 3D acoustic devices for the manipulation of sound reflection. They also show that complex 3D transformation devices can be implemented using present technologies. Given the already reported new improvements in the achievable acoustic material parameters using active metamaterial structures, we expect that the range of realizable transformation acoustics devices will improve markedly in the near future.

Received 9 October 2013; accepted 31 January 2014; published online 9 March 2014

References

1. Pendry, J. B., Schurig, D. & Smith, D. R. Controlling electromagnetic fields. *Science* **312,** 1780–1782 (2006).
2. Leonhardt, U. Optical conformal mapping. *Science* **312,** 1777–1780 (2006).
3. Schurig, D. *et al.* Metamaterial electromagnetic cloak at microwave frequencies. *Science* **314,** 977–980 (2006).
4. Cummer, S. A. & Schurig, D. One path to acoustic cloaking. *New J. Phys.* **9,** 45 (2007).
5. Chen, H. Y. & Chan, C. T. Acoustic cloaking in three dimensions using acoustic metamaterials. *Appl. Phys. Lett.* **91,** 183518 (2007).
6. Cai, W., Chettiar, U. K., Kildishev, A. V. & Shalaev, V. M. Optical cloaking with metamaterials. *Nature Photon.* **1,** 224–227 (2007).
7. Farhat, M., Guenneau, S. & Enoch, S. Ultrabroadband elastic cloaking in thin plates. *Phys. Rev. Lett.* **103,** 024301 (2009).
8. Ergin, T., Stenger, N., Brenner, P., Pendry, J. B. & Wegener, M. Three-dimensional invisibility cloak at optical wavelengths. *Science* **328,** 337–339 (2010).
9. Chen, X. *et al.* Macroscopic invisibility cloaking of visible light. *Nature Commun.* **2,** 176 (2011).
10. Popa, B-I., Zigoneanu, L. & Cummer, S. A. Experimental acoustic ground cloak in air. *Phys. Rev. Lett.* **106,** 253901 (2011).
11. Stenger, N., Wilhelm, M. & Wegener, M. Experiments on elastic cloaking in thin plates. *Phys. Rev. Lett.* **108,** 014301 (2012).
12. Narayana, S. & Sato, Y. Heat flux manipulation with engineered thermal materials. *Phys. Rev. Lett.* **108,** 214303 (2012).
13. Landy, N. & Smith, D. R. A full-parameter unidirectional metamaterial cloak for microwaves. *Nature Mater.* **12,** 25–28 (2013).
14. Schittny, R., Kadic, M., Guenneau, S. & Wegener, M. Experiments on transformation thermodynamics: Molding the flow of heat. *Phys. Rev. Lett.* **110,** 195901 (2013).
15. Zhang, S., Xia, C. & Fang, N. Broadband acoustic cloak for ultrasound waves. *Phys. Rev. Lett.* **106,** 024301 (2011).
16. Cummer, S. A., Rahm, M. & Schurig, D. Material parameters and vector scaling in transformation acoustics. *New J. Phys.* **10,** 115025 (2008).
17. Li, J. & Pendry, J. B. Hiding under the carpet: A new strategy for cloaking. *Phys. Rev. Lett.* **101,** 203901 (2008).
18. Liu, R. *et al.* Broadband ground-plane cloak. *Science* **323,** 366–369 (2009).
19. Valentine, J., Li, J., Zentgraf, T., Bartal, G. & Zhang, X. An optical cloak made of dielectrics. *Nature Mater.* **8,** 568–571 (2009).
20. Garcia-Chocano, V. M. *et al.* Acoustic cloak for airborne sound by inverse design. *Appl. Phys. Lett.* **99,** 074102 (2011).
21. Sanchis, L. *et al.* Three-dimensional axisymmetric cloak based on the cancellation of acoustic scattering from a sphere. *Phys. Rev. Lett.* **110,** 124301 (2013).
22. Li, W., Guan, J., Sun, Z., Wang, W. & Zhang, Q. A near-perfect invisibility cloak constructed with homogeneous materials. *Opt. Express* **17,** 23410–23416 (2009).
23. Zhang, J., Luo, Y. & Mortensen, N. A. Transmission of electromagnetic waves through sub-wavelength channels. *Opt. Express* **18,** 3864–3870 (2010).
24. Weiren, Z., Changlin, D. & Xiaopeng, Z. A numerical method for designing acoustic cloak with homogeneous metamaterials. *Appl. Phys. Lett.* **97,** 131902 (2010).
25. Popa, B-I. & Cummer, S. A. Homogeneous and compact acoustic ground cloaks. *Phys. Rev. B* **83,** 224304 (2011).
26. Zigoneanu, L., Popa, B. I., Starr, A. & Cummer, S. A. Design and measurements of a broadband 2D acoustic metamaterial with anisotropic mass density. *J. Appl. Phys.* **109,** 054906 (2011).

Acknowledgements

This work was supported by Multidisciplinary University Research Initiative grants from the Office of Naval Research (N00014-13-1-0631) and from the Army Research Office (W911NF-09-1-00539).

Author contributions

B-I.P. and L.Z. performed the simulations. L.Z. conducted the fabrication, experimental design and measurements. All three authors equally contributed to the development of the project and to the text of the paper.

Additional information

Supplementary information is available in the online version of the paper. Reprints and permissions information is available online at www.nature.com/reprints. Correspondence and requests for materials should be addressed to S.A.C.

Competing financial interests

The authors declare no competing financial interests.

© 2014 Macmillan Publishers Limited. All rights reserved.